Tunneling study of Fermi-liquid effects in amorphous gallium

G. A. Gibson,* P. M. Tedrow, and R. Meservey
Francis Bitter National Magnet Laboratory, Massachusetts Institute of Technology, Cambridge, Massachusetts 02139
(Received 14 October 1988)

The Fermi-liquid parameter G_0 has been determined in amorphous gallium. $Al/Al_2O_3/a$-Ga tunnel junctions were used to observe the renormalization caused by Fermi-liquid interactions of the spin splitting of the a-Ga superconducting density of states in a magnetic field. This was done by fitting the dynamic tunneling conductance to the theory of Rainer. Excellent agreement was found with this theory, and the results were consistent with critical-field measurements made on the same films. A large renormalization was observed ($G_0=0.81\pm0.14$), as expected for this strongly coupled material. Correlation effects were also seen. The spin-orbit scattering rate b_{SO} was found to be 0.18 ± 0.03.

I. INTRODUCTION

Interaction between the particles of a many-body Fermi system such as a metal or ^{3}He leads to renormalization of many of its equilibrium and transport properties. Fermi-liquid theory[1,2] provides a useful and conceptually economical framework for describing these Fermi-liquid effects (FLE) in terms of just a few parameters. Determination of Fermi-liquid parameters from materials in the normal state is difficult, however, and has only been accomplished for a few elements. For example, conduction-electron spin-resonance absorption[3] and transmission[4–8] experiments, and de Hass–van Alphen[9–12] measurements have been used to measure Fermi-liquid parameters in some of the alkali and noble metals (For a review, see Ref. 13). More recently, by using bilayer samples, Vier *et al.*,[14] have extended the applicability of the transmission technique to include, in principle, all metals for which a conduction-electron spin-resonance signal can be seen. The basic difficulty in determining Fermi-liquid parameters from these measurements is that this requires knowledge of the "bare" quantities, e.g., the effective mass in the absence of Fermi-liquid effects. Fermi-liquid theory deals with the residual interaction between already dressed quasiparticles. In real metals the electrons will interact, for example, with phonons, thereby changing their effective mass. There will also often be an orbital contribution to the susceptibility. Thus, in all but the simplest metals, it is difficult to know how much of the measured renormalization is due to Fermi-liquid interactions. The superconducting tunneling experiment described here avoids this problem, as it is sensitive only to the Fermi-liquid renormalization.

The need to include FLE in the description of superconductivity was first pointed out by Clogston.[15] Experimental support for this was provided by the unphysically large values of the spin-orbit scattering rate needed to fit the critical field H_{c2} measurements of Orlando and coworkers on $A15$ superconductors.[16,17] To obtain more reasonable fits to their data, these authors found it beneficial to include FLE. The inadequacy of the unrenormalized theory[18–21] became even clearer when it was compared to tunneling and critical-field data on Al thin films.[22,23] Tedrow *et al.*[24] showed that for Al thin films their spin-polarized tunneling and critical field [$H_{c2}(T)$] data could be explained using a generalized theory by Rainer[25] which includes FLE. One result of these experiments was to demonstrate a new and very direct way of measuring the Fermi-liquid renormalization in metals. The great advantage in using a superconductor for such measurements is that along a second-order phase boundary, $H_{c2}(T)$, the densities of quasiparticles in the normal and superconducting states are equal, but for $H \ll H_{c2}(0)$ and $T \ll T_c$ the density of the unpaired quasiparticles approaches zero, and the interaction between quasiparticles is effectively turned off. Thus we can separate the renormalization of the quasiparticles[26] due to Fermi-liquid interactions from the effects which "dress" the noninteracting quasiparticles, by varying the magnetic field and temperature. The present measurements utilize this property of superconductors to determine Fermi-liquid parameters without relying on model calculations or other experiments to determine the bare quantities.

According to the theory, the rather modest Fermi-liquid correction observed in Al (Ref. 24) should be greatly exceeded by that of a superconductor with a large electron-phonon coupling constant ($\lambda_{e\text{-ph}}$). The value of $\lambda_{e\text{-ph}}$ for amorphous gallium (a-Ga) (Refs. 27–29) is $\simeq 2$ compared with a value of $\simeq 0.4$ for Al.[30] It also has a sufficiently low spin-orbit scattering rate for the present experiment, unlike other strongly coupled superconductors. Quench-condensed a-Ga films have been extensively studied[27,28,31–38] in spite of the fact that they are only stable for $T \leq 20$ K and must be prepared by deposition on a substrate held at liquid-helium temperature. High-T_c modifications have been produced by other techniques but these generally include phases with a lower T_c and $\lambda_{e\text{-ph}}$.[32,39,40] We have observed a large renormalization of the superconducting density of states and critical field of a-Ga, underscoring the need to incorporate Fermi-liquid

effects in understanding the superconducting behavior of this material and providing a rigorous test of the renormalized theory.

II. THEORY

Near a second-order phase transition to the normal state, the density of quasiparticles approaches the normal-state density of electrons, and interaction between them becomes important. The effect of the neighboring quasiparticles on a given quasiparticle can be described in terms of an additional magnetic field acting on its spin (in addition to the renormalization of its self-energy or effective mass). Since this extra field is equivalent to renormalizing the effective magnetic moment of the quasiparticle, the interaction renormalizes the superconducting properties dependent on this moment, such as the Pauli-limited critical field and the spin-splitting of the quasiparticle density of states in a magnetic field. The present study is based on these effects.

The theoretical foundation for the application of Fermi-liquid[1,2] theory to isotropic superfluids in the clean limit was laid by Leggett.[41–43] We will use the quasiclassical approach developed by Eilenberger[44] and Larkin and Ovchinkov.[45] This approach has been used by Serene and Rainer[46] to describe ^{3}He. The extension of this theory to high-field superconductivity used here is due to Rainer.[25] The high-field properties of superconductors, in particular the superconducting density of states and upper critical field, are calculated from the quasiclassical propagator for the quasiparticle excitations. Impurity, anisotropy, and strong-coupling effects can all be incorporated. We are interested in the dirty limit ($l \ll \xi_0$) for our amorphous films, where the quasiparticle parameters can be averaged over the Fermi surface. It is important to note that in the dirty limit the renormalization of both the quasiparticle density of states and the critical field is characterized by the singe parameter G_0. This is the $l=0$, antisymmetric, Fermi-liquid parameter which is sometimes referred to as B_0 in the literature.

In the limit where the interaction of the applied magnetic field with the spins dominates the coupling between the orbital motion and the field (e.g., a thin film in a parallel field where the orbital depairing is negligible) the renormalization of the Pauli-limited field (H_p) is given by,[15,16]

$$H_p = H_p^0(1+G_0) \ . \tag{1}$$

We also find from this theory that as the applied field approaches the critical field, the apparent Zeeman splitting, δ, of te quasiparticle excitations becomes

$$\delta \xrightarrow{H(T)\to H_c(T)} 2\mu_B H_c(T)/(1+G_0) \ . \tag{2}$$

From these relations, we see that at the phase boundary the effect of the interaction between quasiparticles is equivalent to adding an extra internal field,[47] $H_{\rm int}=H_{\rm ext}[-G_0/(1+G_0)]$, which acts on the quasiparticles' spins (in addition to renormalizing their masses). This field can be either positive or negative depending on the sign of G_0.

It is difficult to determine G_0 from critical field measurements alone. This point has been discussed in detail by Alexander.[48] The problem is that spin-orbit scattering has an effect on the critical field which is very similar to that of the renormalization. This spin-orbit scattering is analogous to that in the simple hydrogen atom problem. Grain boundaries, impurities, defects, and interfaces can all lead to potentials which yield an "$\mathbf{L}\cdot\mathbf{s}$" coupling term in the Hamiltonian. In the theory used here, these effects are combined together into a single phenomenological spin-orbit (SO) scattering time, $\tau_{\rm SO}$. The spin-orbit scattering rate, $b_{\rm SO}=\hbar/3\tau_{\rm SO}\Delta_0$, will be an additional fitting parameter in the theory (Δ_0 is the order parameter of the superconductor in the absence of any pairbreaking). The best way to determine G_0 is by fitting curves calculated using the theory of Rainer to measured conductance curves. In a superconductor–normal metal tunnel junction, the dynamic conductance as a function of bias voltage is simply the convolution of the superconducting density of states, $N_s(V)$, with the derivative of the Fermi function with respect to energy.[49] The full effect of G_0 on the shape of $N_s(V)$ is complicated and depends on the amount of orbital depairing and the spin-orbit scattering rate in the superconductor. One of the main features of the renormalization is a decrease in the apparent Zeeman splitting. The change in this splitting as a function of field can be measured directly and compared with that predicted by the theory in order to determine G_0 when the spin-orbit scattering rate is low. This approach has been used by Tedrow *et al.*[24] on aluminum, which has a very low spin-orbit scattering rate. They used $Al/Al_2O_3/Fe$ tunnel junctions to resolve the two quasiparticle spin densities of states of the aluminum. This technique has been described by Meservey *et al.*[37] and Tedrow *et al.*[50] By measuring the separation in energy of these densities of states, Tedrow *et al.*[24] obtained $G_0=0.3$.

With a moderate amount of spin-orbit scattering, spin is no longer a good quantum number but G_0 can be accurately determined by fitting the full energy dependence of the quasiparticle density of state to the theory. In this way, the effect of spin-orbit scattering is properly taken into account. Although both spin-orbit scattering and the renormalization (for $G_0>0$) tend to reduce the apparent Zeeman splitting, their exact effect on the superconducting density of states as a function of energy is not the same. This will become clearer when we fit the conductance curves for amorphous gallium tunnel junctions. Alexander *et al.*[25] and Alexander[48] fitted the full superconducting density of states for aluminum and again got $G_0\sim 0.3$.

Our expectation in studying amorphous gallium was to observe a large renormalization, because of its strong electron-phonon coupling ($\lambda_{e\text{-ph}}\simeq 2$). While there are other superconductors with large electron-phonon coupling constants, such as PbBi, most consist of high atomic number elements and consequently have spin-orbit scattering rates which are too large to allow this study (see discussion section). As we shall see, the spin-orbit

scattering rate in amorphous gallium is moderate ($b_{SO} \simeq 0.18$), and we use a full fit of the density of states in determining G_0. The large size of the renormalization allows it to be unambiguously distinguished from the similar effects of spin-orbit scattering, which is difficult in the case of aluminum. The large renormalization also provides a rigorous test of Rainer's theory. For an excellent review of high-field superconductivity in the absence of Fermi-liquid effects see Fulde.[20]

III. APPARATUS AND EXPERIMENTAL PROCEDURE

The major experimental difficulty involved in working with amorphous gallium tunnel junctions is that the Ga must be deposited at liquid-helium temperature and the junctions tested *in situ*. This is necessary both because amorphous gallium anneals to a more ordered phase at approximately 20 K and because the extremely thin films which are required in the present study oxidize rapidly in air. In addition, magnetic fields of the order of 20 T are required. A low-temperature evaporator which can be operated within a 2-in.-bore Bitter magnet was used. This device is shown schematically in Fig. 1. A stainless-steel cryogenic dewar is supported just above the magnet. The "tail" section of the dewar has been lengthened and is inserted through the bore of the magnet. The end of the "tail" section is clamped to a metal bellows attached to a vacuum chamber which lies below the magnet. This allows removal of the system from the magnet. Thermal evaporation sources are mounted on a removeable flange at the bottom of the vacuum chamber. The evaporation boats are surrounded by a liquid-nitrogen cooled shield with an opening at the top. A shutter is positioned above this opening and can be controlled from the outside by a rotary feedthrough. A quartz crystal rate monitor views the source through a second hole in the liquid-nitrogen shield. The vacuum spaces between the liquid nitrogen and liquid helium are connected with each other as well as the vacuum chamber below the magnet. This single vacuum space is pumped by a cryopump mounted directly on the side of the vacuum chamber next to the evaporation sources. When the system is fully cooled, the pressure at the ion gauge is less than 10^{-7} torr. The pressure at the sample, which is completely surrounded by surfaces at ~ 1 K or less, is no doubt considerably lower. A ^{3}He pot is attached to a pumping tube which runs up through the ^{4}He chamber (see Fig. 1). The sample substrate is mounted on a rotatable stage which is thermally anchored to the ^{3}He pot. The sample stage can be rotated from the outside so as to face down toward the source during deposition and then aligned parallel with the field for measurements. The sample is surrounded by a copper radiation shield which is mounted on the bottom of the pumped ^{4}He bath. This, in turn, is surrounded by an aluminum radiation shield which is thermally anchored to the bottom of the liquid-nitrogen bath. There is a $\frac{3}{8}$-in. opening at the bottom of each shield for the passage of the evaporant. This pathway can be blocked by a shutter which is thermally anchored to the ^{3}He pot. A mask can be attached to the sample holder so as to produce the desired pattern. By pumping on the ^{3}He bath, temperatures as low as 0.7 K could be achieved.

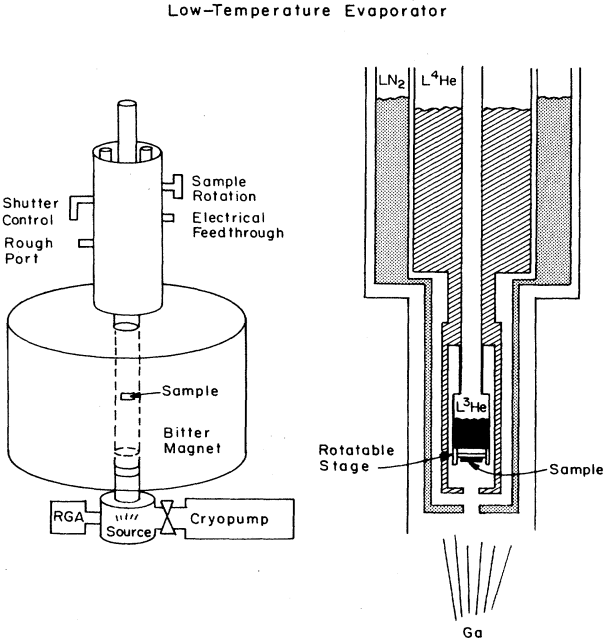

FIG. 1. Schematic view of low-temperature evaporator used to make Al/Al_2O_3/a-Ga tunnel junctions (left). Cross-sectional view of modified Janis dewar in which sample was mounted.

The following procedure was used to form the tunnel junctions. Gold contacts were evaporated onto liquid-nitrogen-cooled glass substrates in a separate evaporator [see Fig. 2(a)]. These were then counted in the low-temperature evaporator, and leads were attached to the gold contacts with pressed indium. The sample was again cooled to liquid-nitrogen temperature by putting liquid nitrogen in the ^{3}He compartment. Approximately 300 Å of aluminum were evaporated in order to complete the "cross-strips" [see Fig. 2(b)]. The system was then warmed to room temperature and the mask changed. In the process the aluminum was exposed to air for between 15 min and 1 h. This exposure oxidized the top surface of the aluminum and formed a tunnel barrier. The system was evacuated, cooled to the lowest possible temperature, and the gallium evaporated, forming two tunnel junctions [see Fig. 2(c)]. Note that four-terminal measurements of the gallium "long-strips" could also be made. The gallium films were made as thin as possible in order to minimize their orbital depairing in a field. This was accomplished by slowly depositing the gallium while monitoring the electrical continuity of the film. The films generally became continuous at approximately 15 Å, but evaporation was continued until they reached about 20–25 Å. Thinner films usually did not survive long and had unmanageably low critical currents. During the gallium evaporation, an aluminum film with a T_c of 2.3 K

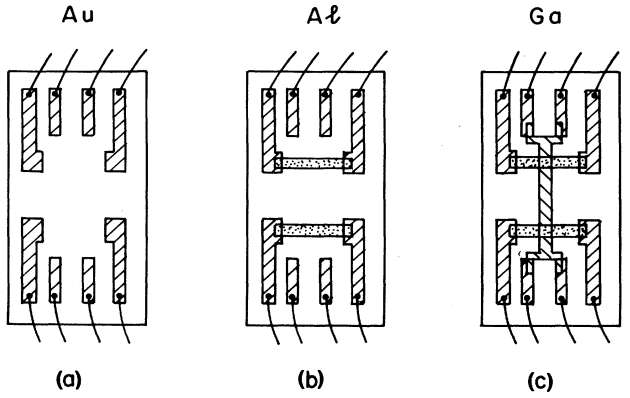

FIG. 2. Three steps in the production of $Al/Al_2O_3/a$-Ga tunnel junctions. (a) Evaporation of gold contacts onto $\frac{1}{4}$-in.$\times\frac{1}{2}$-in. glass substrates in separate evaporator. (b) Evaporation of aluminum "cross-strips" at 77 K in low-temperature evaporator. (c) Completion of two tunnel junctions by evaporation of gallium "long-strip" at ≤ 2 K.

remained superconducting and showed that the temperature of the glass was low enough for the gallium to be amorphous.

The junctions were aligned parallel to the field by maximizing the critical field of the aluminum strip. The aluminum was used because the parallel critical field of the gallium films was often greater than the available field of 20 T. The dynamic conductance of the tunnel junctions as a function of voltage was measured for various fields and temperatures. Finally, the critical field was measured at as many temperature points as possible.

IV. ANALYSIS OF TUNNELING DATA

The dynamic conductance versus bias voltage for a typical $Al/Al_2O_3/a$-Ga tunnel junction at zero field and low temperature is shown in Fig. 3. The leakage current is negligible and the features are quite sharp, indicating that tunneling is the primary conduction process and that the films are uniform and of high quality. At this low temperature and zero magnetic field, the aluminum is also superconducting, as shown by the very sharp conductance peaks at $\pm(\Delta_{Al}+\Delta_{Ga})$. The difference peaks are not observed because not many quasiparticles are excited at low temperature. In Fig. 4 we see a similar junction at a higher temperature where both the sum and difference peaks are observable. This curve gives an additional measure of the gap in both the aluminum and gallium. The normal-state tunneling resistance of these junctions ranged between 20 and 100 kΩ.

The transition temperature of the gallium films, measured resistively, varied from 6.8 to 7.7 K. These values are somewhat lower than for thick-film amorphous gallium, which has a T_c of about 8.4.[27,28,31,33,35,37] A lowered transition temperature is a common feature of superconducting thin films and has been observed previously in amorphous gallium. Naugle and Glover[35] found a d^{-1} dependence of T_c on thickness consistent with the present result. The resistivities of the gallium films were in the range of 75 to 200 $\mu\Omega$ cm. There is an uncertainty of about a factor of 2 in the resistivity measurements due to the geometry of the films. The parallel critical fields of these films at low temperature were typically at the limit of the magnet, or just slightly more than 20 T. The perpendicular critical fields ranged from 11 to 13 T. One very thin film ($\simeq 15$ Å) had a perpendicular critical field of 15 T.

We fit our tunneling data using a program written by Rainer based on his extension of the theory of high-field superconductivity[18–20] to include Fermi-liquid interactions.[25] The input parameters to the theory are the Fermi-liquid parameter G_0, the spin-orbit scattering rate b_{SO}, two orbital-depairing parameters, and the measured transition temperature. Theoretically, the orbital depairing for a thin film in a parallel field should be proportional to the square of the field.[19,20] We find that in order to

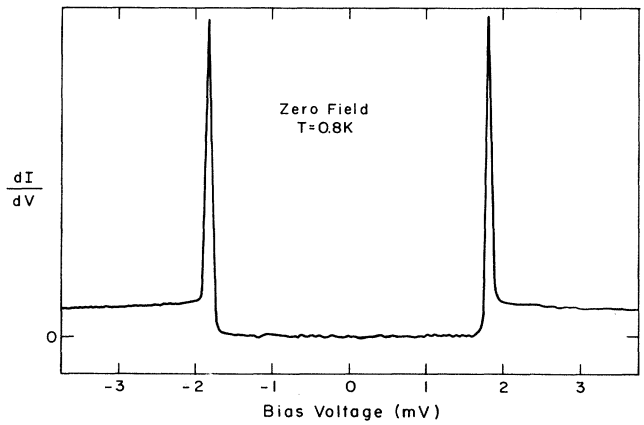

FIG. 3. Dynamic conductance vs bias voltage for a typical $Al/Al_2O_3/a$-Ga tunnel junction at $H=0$, $T=0.8$ K. At this low temperature only the "sum" peaks are observed.

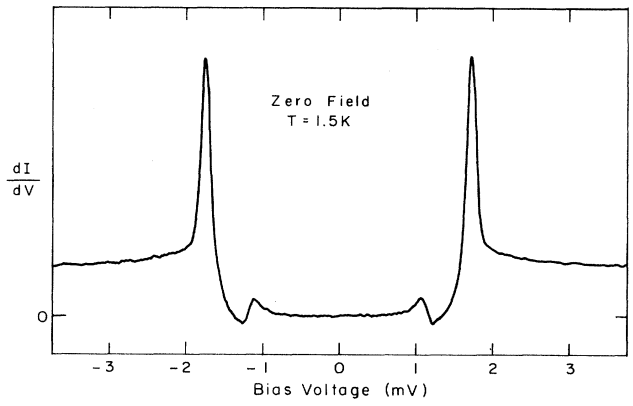

FIG. 4. Dynamic conductance at $H=0$, $T=1.5$ K. At this temperature both the sum and difference peaks are observed.

get the best fit to the data we must include a pair-breaking term, P_0, which is independent of field. This has also been found to be the case for tunneling data on aluminum[37] and vanadium.[51] It may in part be due to overmodulation of the junction by noise. A further possibility is quasiparticle lifetime broadening due to quasiparticle recombination[52] or correlation effects.[53] This lifetime broadening partially mimics the effect of pair breaking on the superconducting density of states. The theory for the behavior of the superconducting density of states in the presence of correlation effects has been developed by Browne *et al.*[54] To describe the H^2 depairing term we will use Fulde's depairing parameter,[20] $c_F = De^2d^2\Delta 0/\mu_B^2\hbar c^2$. Here $D=lv_F/3$ is the diffusion constant with l the transport mean free path and v_F the Fermi velocity. The total pairbreaking is given by

$$P=\left[\frac{k_B T_{c0}}{\Delta_0}\right]c_F h^2+P_0 ,$$

where P_0 is the zero-field depairing parameter, T_{c0} is the transition temperature in the absence of all pairbreaking, and $h=\mu_B H/k_B T_{c0}$. As defined here, $P-P_0$ is the square of the ratio of the orbital to spin energy differences between time-reversed states. Typically we found $P_0 \sim 0.05-0.10$ and $c_F \sim 0.3$. This small value for P_0 has negligible effect on the value we determine for G_0.

Rainer's program, as written, does not explicitly include strong coupling. We have approximated its effect by simply multiplying the gap by $(2\Delta/kT_{c0})/3.52$ wherever it appears, as suggested by Rainer. For all five of the junctions measured, it was found that using $2\Delta/kT_{c0}=4.45$ produced very good fits to the data. This value is very close to those reported by others.[27,32–34]

In comparing theoretical curves with data, first, a conductance curve obtained for an applied field just above the critical field of the aluminum electrode ($H_c \simeq 4$ T) was fitted. At this low field the effects of the renormalization, spin-orbit scattering, and the H^2 part of the orbital depairing were negligible. Thus, the only adjustable parameter was P_0. After determining P_0, higher field curves were used to determine c_F, b_{SO}, and G_0. First, c_F was determined by roughly fitting the size of the gap at high fields. Then b_{SO} and G_0 were determined by fitting the full shape of the curve. The effect of increasing the spin-orbit scattering rate of the renormalization is illustrated in Fig. 5. It can be seen that, while both decrease the apparent splitting, the overall change in the shape of the density of states is not exactly the same. For example, increases in b_{SO} result in larger relative increases in the height of the "shoulder" at the positions of the inner peaks. Thus, by carefully fitting the full shape of the conductance curves, it is possible to distinguish the effects of the renormalization and spin-orbit scattering and to determine accurately both G_0 and b_{SO}. This fact is further illustrated in Fig. 6. Here, the solid curves are data taken on a single junction at two different fields. The dashed lines are a fit to these data. The same parameters were used to fit both curves as well as others taken on the same junction at different fields and temperatures. The values $G_0=0.67$, $b_{SO}=0.21$, $c_F=0.235$, and $P_0=0.055$

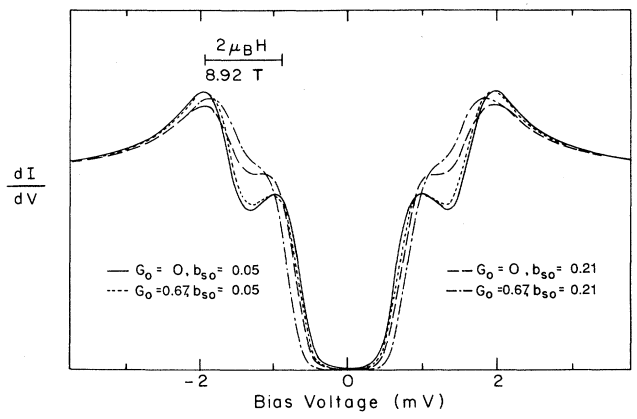

FIG. 5. The solid curve is the prediction of Rainer's theory for $G_0=0$, $b_{SO}=0.05$. The dotted curve is that predicted for $G_0=0.67$, $b_{SO}=0.05$. The dashed curve corresponds to $G_0=0$, $b_{SO}=0.21$ and the dash-dot curve is for $G_0=0.67$, $b_{SO}=0.21$.

provide a very good fit to all the experimental curves (see middle figure in both columns). Now if we arbitrarily hold G_0 fixed at 0.33 and vary the other parameters to get the best fit simultaneously for all the curves, the best we can do is shown in the bottom figures. Similarly, if we fix G_0 at too large a value, say 1.2, the best fit we have managed is shown in the top figures. This clearly shows that the effects of the renormalization and spin-orbit scattering can be distinguished. It also provides a measure of the accuracy with which we can determine G_0. With good data, such as those shown, careful fitting can determine G_0 to within better than 20%.

Figure 7 shows conductance curves at a number of fields for a single junction. Again, the dashed curves are a fit to the theory of Rainer using a single set of parameters. A very good fit is obtained over the entire range of magnetic field. The increasing discrepancy near zero-bias is a common feature of tunneling conductance fits in high fields.[25,38,48,51] Here it may be due in part to a slight misalignment of the junctions in the field. The discrepancy has also been attributed to lifetime broadening effects.[48]

There is also an increasing difference between the experimental curves and the theory at voltages above the gap. This background curvature cannot be attributed to an increasing tunneling probability with increasing voltage. Al_2O_3 barriers are on the order of 2 eV high and should not cause any curvature at these low biases. Also, the sign of the observed curvature is the opposite of what one would expect from a low barrier. We believe instead that this background is due to electron correlation effects. The gallium films are very thin (~20–25 Å) and highly disordered. Consequently, the electrons' motion is diffusive, screening is reduced, and the Coulomb interaction is enhanced. From the large resistivity of our gallium films we estimate that $k_F l$ is only ~3–10. Note that the resistivity (75–200 $\mu\Omega$ cm) is significantly larger than the values of 26–34 $\mu\Omega$ cm reported for amorphous gallium films over 150 Å thick.[29,35,55] For a three-

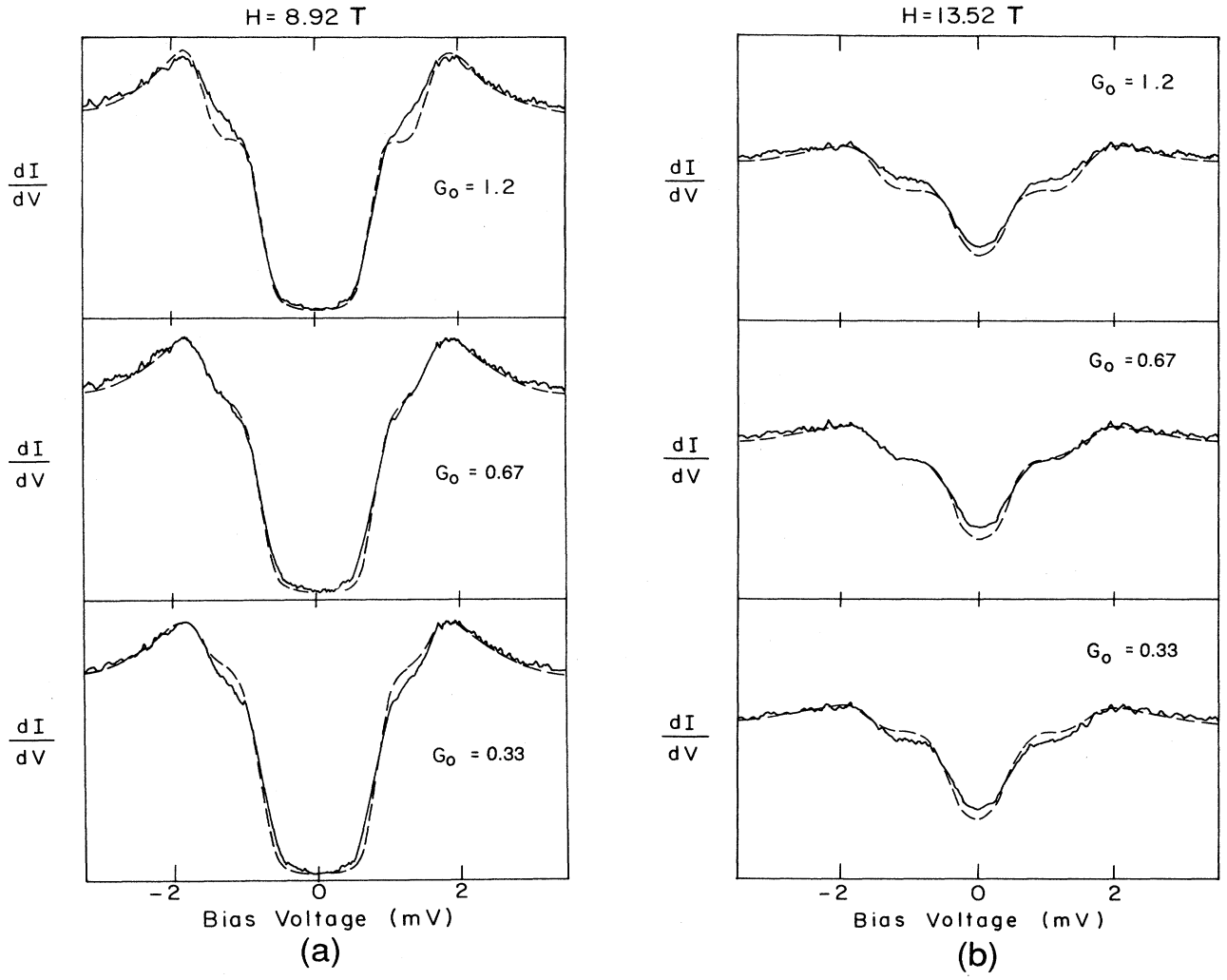

FIG. 6. (a) Solid curve in each part is experimental data taken at 8.92 T. Dashed curves are best fits obtained for these data while simultaneously fitting all the data taken on this junction at other fields and temperatures. In each of the three cases G_0 was held fixed at the indicated value while the other parameters were allowed to vary. (b) Same thing for an experimental curve from the same junction taken at 13.52 T.

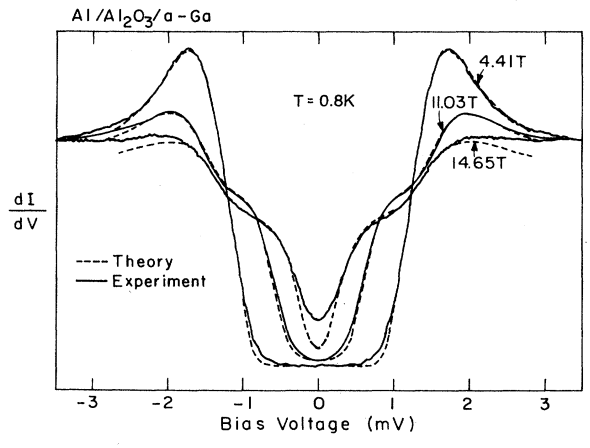

FIG. 7. Conductance curves at three different fields for a single junction. Dashed curves are a fit to the theory of Rainer with $G_0=0.82$, $b_{SO}=0.16$, $c_F=0.325$, and $P_0=0.11$. $T_{c0}=8.4$.

dimensional sample it has been shown that correlation leads to a cusp in the normal state density of states,[56,57]

$$N(E)=N(0)\left[1+\left[\frac{E}{\Delta}\right]^{1/2}\right], \tag{3}$$

where E is the energy measured from the Fermi level and Δ is the correlation gap. In two dimensions the singularity becomes logarithmic in the energy.[58] Two-dimensional behavior is expected when the sample thickness is less than both $(\hbar D/eV)^{1/2}$ and $(\hbar D/kT)^{1/2}$ where D is the diffusion constant. The resistivity of the aluminum electrodes is low ($\sim 10\ \mu\Omega$ cm) so that we do not expect to observe correlation effects in them. In fact, junctions with similar aluminum electrodes used in other studies do not show any background curvature. Thus, the density of states of the aluminum electrode should be constant over this energy range and the dynamic conductance of the junction should be proportional to the density of

states of the gallium. In Fig. 8 we show the dynamic conductance for one of our amorphous gallium junctions above the transition temperature of the gallium. A square-root dependence on energy is clearly seen. The slight deviation at low energy is due to overmodulation of the junction, which tends to round out the cusp at low bias. We have also observed the logarithmic energy dependence in very thin films of amorphous gallium (as well as quench-condensed vanadium and palladium) at low temperature and bias. This work will be reported elsewhere.[51] In any case, we have eliminated the measured background conductance from the data and compared the result with the theory. First a straight line was fitted to dI/dV versus $V^{1/2}$ at voltages well above the superconducting energy gap for $T=0.9$ K and $H=0$. Then this function was divided out of all the measured curves regardless of T and H. Above the gap there appeared to be negligible change in the background curvature in the range of field and temperature used in this experiment: 0–20 T, 0.8–3.5 K. At voltages below the gap, it is difficult to determine the effect of the field and temperature because of the superconducting energy-gap. The result of performing this division for the junction used in Fig. 7 is shown in Fig. 9. The horizontal bar in this figure represents the value of $2\mu_B H$ for the 14.65 T curve. The observed splitting is significantly less than this due to the Fermi-liquid interaction. Note that for all our junctions, dividing out the background makes negligible difference in the value obtained for G_0 (over the range of voltage examined, the change in normal state conductance changed typically by only 10–30 %).

Figure 10 shows how, at the highest fields, the depairing becomes too large to observe the splitting. Here again the background observed at zero field has been removed. In most of the junctions the Zeeman splitting of the quasiparticle excitations became indiscernable at about 17 T. The highest field at which splitting was observed was 17.2 T. The parameters used to fit the curves

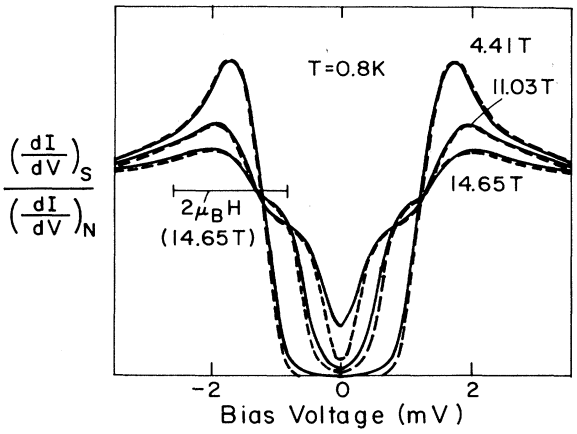

FIG. 9. Data of Fig. 7 with measured background conductance divided out. The horizontal bar represents $2\mu_B H$ at 14.65 T. The splitting observed at this field is clearly much less than $2\mu_B H$.

in Fig. 10 also gave an excellent fit to lower field curves taken on the same junction. Figure 11 shows the effect of holding the field constant while raising the temperature. The data here are from the same junction shown in Figs. 7 and 9. A good fit to the data is obtained using the same set of parameters used in those figures.

In all, the data from five junctions were fitted to the theory of Rainer. The results are summarized in Table I. As can be seen, the results are quite consistent from junction to junction. We obtain the values $G_0=0.81\pm0.14$ and $b_{SO}=0.18\pm0.03$. Critical-field data were also taken on some of the gallium films. The data points shown in Fig. 12 were taken on the gallium electrode of the junction used in Figs. 7 and 9. The solid curve is the theoretical prediction for the critical field derived by using the values obtained from the tunneling data for c_F, P_0, b_{SO},

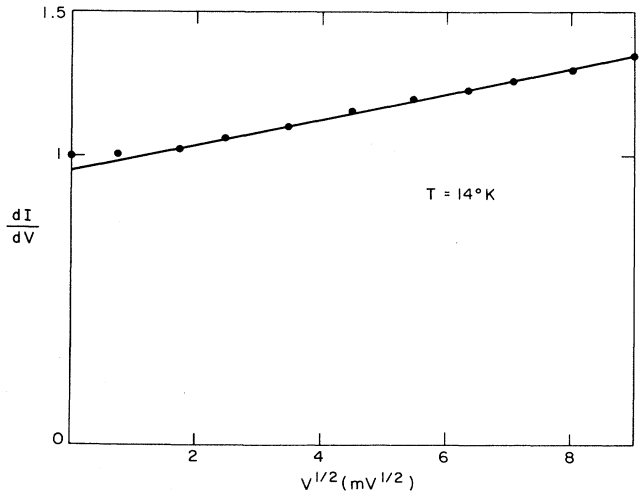

FIG. 8. Dynamic conductance of junction with gallium normal. Shows $V^{1/2}$ dependence as in Eq. (3).

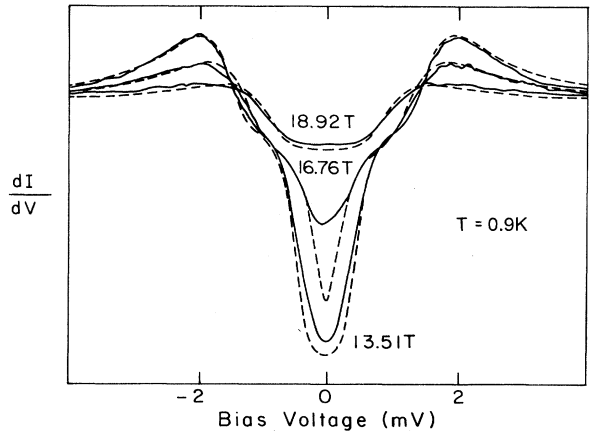

FIG. 10. Dynamic conductance at high fields. Solid curves are experimental and dashed lines are a fit to Rainer's theory using $G_0=0.818$, $b_{SO}=0.19$, $c_F=0.35$, and $P_0=0.04$. Above 17.2 T splitting could not be observed in any of the junctions studied due to the large depairing.

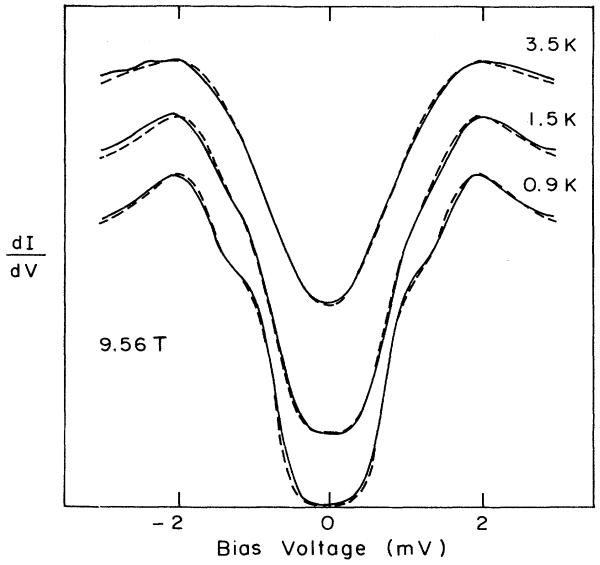

FIG. 11. Temperature dependence of conductance. Solid curves are experimental data on the same junction shown in Figs. 7 and 9. Dashed lines are the prediction of Rainer's theory for the same parameters used in those figures.

and G_0. The agreement between the tunneling data and the critical-field data is quite good. There is some uncertainty in the temperature of the data points taken above 2 K because of the difficulty in stabilizing the temperature of the sample without ^{3}He condensed in the ^{3}He pot. Between 2 and 4.5 K there are no data points because of the extremely rapid fluctuations of the temperature in this range. The higher temperature points were taken by holding the field constant and letting the temperature slowly drift through $T_c(H)$.

Recall that $2\Delta_0/KT_c \simeq 4.45$ for amorphous gallium and that the theory used is a weak-coupling theory. Rainer *et al.*[59] have calculated the critical field for $Pb_{0.75}Bi_{0.25}$ using the full $\alpha^2F(\omega)$ dependence on frequency. They find that the bulk critical field is enhanced at low temperature by 10% to 20% over the weak-coupling calculation (depending on the spin-orbit scattering rate). The phonon spectral density of $Pb_{0.75}Bi_{0.25}$ is similar to that of amorphous gallium.[36] Thus, a strong-coupling calculation of the critical field for our gallium films should bring the prediction into closer agreement with the data at low temperature.

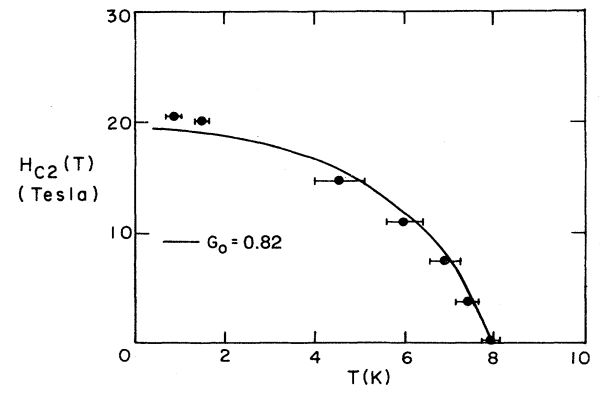

FIG. 12. Critical-field data for gallium film of junction used in Figs. 7 and 9. The solid curve is the prediction of Rainer's theory using the parameters obtained from the tunneling data. ($G_0=0.818$, $b_{SO}=0.16$, $c_F=0.325$, and $P_0=0.11$).

TABLE I. Fitting parameters for five best junctions.

Junction	G_0	b_{SO}	c_F	P_0	T_c	T_{c0}
1	0.724	0.17	0.17	0.155	7.22	8.25
2	0.667	0.21	0.235	0.055	7.27	7.6
3	0.818	0.19	0.35	0.04	7.75	8
4	0.818	0.16	0.325	0.11	7.66	8.4
5	0.95	0.16	0.13	0.07	6.8	7.2

V. DISCUSSION

In this section we will discuss the applicability of the theory and the reasonableness of our result for G_0. We will also compare this result to that predicted by Eq. (4).

In the limit where correlation effects become very large, Fermi-liquid theory will break down. In our films the change in the normal-state conductance was only $\sim 10-30\%$ over the range of voltage studied. The presence of only a small change in the normal-state density of states due to correlation indicates that the Fermi-liquid theory remains valid.

The effective coherence length at $T=0$ we get from the perpendicular critical field is

$$\xi_{\text{eff}} = \left[\frac{\Phi_0}{2\pi H_{c2}^{\perp}}\right]^{1/2} \sim 35\ \text{Å} \geq d\ ,$$

so we are correct in taking the thin film, parallel field limit, of the theory. Here $\Phi_0 = hc/2e$ is the magnetic flux quantum. That we are in the two-dimensional (2D) limit can also be seen from the fact that the parallel critical field is much larger than the perpendicular one, $H_{c\parallel}(0)/H_{c\perp}(0) \sim 1.67$.[60] Furthermore, we are clearly in the dirty limit, which allows us to average the quasiparticle parameters over the Fermi surface and justifies the use of only the isotropic Fermi-liquid parameter G_0 in describing the renormalization.

To incorporate strong coupling, we simply multiplied the gap by a constant factor wherever it appeared in the theory, as described in Sec. IV. A full strong-coupling calculation, including the energy dependence of the interaction, would be considerably more complicated. To include higher-order terms in T_c/Θ_D would require defining "higher-order" Fermi-liquid parameters, as the mean-field potential seen by the quasiparticles would no longer be a linear functional of the quasiparticle propagator. We can view our result as an effective, first-order (in T_c/Θ_D), Fermi-liquid parameter. Again, this is not a large effect.

Finally, we conclude that the Fermi-liquid theory, as used here, explains quite well the renormalization of the density of states in amorphous gallium, as both a function

of temperature and field. Also, the parameters obtained from this theory are consistent from sample to sample.

The value obtained for G_0, 0.81 ± 0.14, is somewhat less than one would naively expect for an electron-phonon coupling constant $\lambda_{e\text{-ph}}\simeq 2$. We will now compare our result for G_0 with that predicted by the following simple relation:

$$1+G_0=(1+\lambda_{e\text{-ph}}+\lambda_s)(1-\bar{I})\ , \tag{4}$$

where λ_s is the mass renormalization due to spin fluctuations (paramagnons), and $(1-\bar{I})^{-1}$ is the Stoner factor.[61] This equation has been suggested[62] as the proper way to determine the net renormalization when both electron-phonon and paramagnon enhanced electron-electron interactions are important. To our knowledge, the Stoner factor and the electron-electron mass enhancement, λ_s, have not been determined from amorphous gallium. However, we can make the following crude estimate. Chen *et al.*[27] have measured the Eliashberg function, $\alpha^2F(\omega)$, for *a*-Ga and inverted it to obtain $\lambda_{e\text{-ph}}2.25\pm0.2$ and $\mu^*=0.17\pm0.02$, where μ^* is the Coulomb pseudopotential. Similarly, Jackson *et al.*[28] have obtained $\lambda_{e\text{-ph}}=1.94$ and $\mu^*=0.15$. These are unusually large values for μ^*. One would expect a value more like 0.11,[63] which is what Chen *et al.* obtained for quenched-condensed bismuth.[27] They found, however, that 0.17 gave a very good fit while 0.1 yielded a poor fit. The high value may be the result of the rescaling due to paramagnons described by Daams *et al.*[64] This interpretation would indicate a value for $\lambda_s\simeq 0.05-0.07$. The exact value of λ_s makes little difference in Eq. (4) as it is small in any case. Jensen and Andres[65] have shown that a crude approximation for the Coulomb exchange potential is that it is three times the Coulomb pseudopotential. Thus,

$$\bar{I}\sim N(0)\bar{V}_c\sim 3N(0)\bar{U}_c=3\mu^*\simeq 0.48\ . \tag{5}$$

If we use these numbers in Eq. (4) we get,

$$1+G_0\simeq 1.64\ .$$

This is close to the measured result. Leavens and MacDonald[66] argue that Eq. (4) is only good when the exchange enhancement factor is large. The large measured value for μ^* and our relatively small value for G_0 indicate that this may be the case. Rainer[67] has also pointed out that it is not conceptually correct to try to separate the net renormalization into its constituent interactions. However, for amorphous gallium, and aluminum and vanadium,[51] Eq. (4) seems to predict values for G_0 consistent with our data. Thus, it seems possible to predict the overall renormalization by simply summing the contributions from the electron-electron and electron-phonon interactions in this way.

This conclusion is, of course, contingent on whether the value for G_0 obtained from these thin films is applicable to thicker films ("bulk"). The fact that the T_c's are somewhat reduced indicates that there is probably some change in the phonon spectral density and/or the density of states. However, the reduction in T_c is only 10–20 % so we do not expect this thickness dependence to be a large effect.

As a final note, we consider our measured value for the spin-orbit scattering rate, $b_{SO}=0.18\pm0.03$. We can make a rough estimate for b_{SO} using the formula derived by Gallagher[68] using Fermi's Golden Rule

$$\hbar/\tau_{SO}\sim 2\pi c[\Omega D(E_f)]|\Delta_{SO}|^2\ . \tag{6}$$

Here c is the fractional concentration of spin-orbit scattering centers (defects, impurities, etc.), $D(E_F)$ is the density of states at the Fermi level, Ω is the volume of the unit cell, and Δ_{SO} is the matrix element for spin-orbit scattering. Note that since $\Delta_{SO}\sim Z^2$ where Z is the atomic number of the scatterer,[69,70] that Eq. (6) gives the relation $b_{SO}\sim Z^4$ suggested by Abrikosov and Gorkov.[71] For Δ_{SO}^{Ga} we will use the value 0.102 meV obtained by Yafet.[72] If we make the assumption that all the spin-orbit scattering in these film occurs at the surface[73] and that every surface atom causes scattering, then $c\sim 1/d$, where d is measured in lattice constants. Using the bulk values for crystalline gallium for the lattice constant (2.69 Å), and k_F (1.65×10^8 cm^{-1}), we can calculate Ω (19.6 Å^3), c (0.067), and

$$D(E_F)=mk_F/2\pi^2\hbar^2\simeq 8.4\times10^{33}\ \text{states/erg cm}^3$$

(using the free-electron model and the bare electron mass[74]). From this we get $\hbar/\tau_{SO}\simeq 1.1$ meV. Thus, $b_{SO}=\hbar/3\tau_{SO}\Delta_0\simeq 0.25$. This is close to the measured value of 0.18. A similar analysis for thin aluminum films yields a value of $b_{SO}\simeq 0.12$. This is also somewhat more than the value ($\simeq 0.05$) obtained from tunneling.[25] In short, our measured spin-orbit scattering rate is consistent with the simple calculation and with measurements on other superconductors. A more complete discussion of spin-orbit scattering in superconductors may be found elsewhere.[67,75]

VI. SUMMARY

We have found good agreement between Rainer's theory, which incorporates Fermi-liquid effects into the high-field theory of superconductivity, and our tunneling data on amorphous gallium. This agreement demonstrates the accuracy of the theory when the net Fermi-liquid interaction is large. This interaction manifests itself in a large renormalization of the quasiparticle density of states. The change in this density of states as a function of both temperature and magnetic field was fitted with a single set of values for the depairing, spin-orbit scattering, and Fermi-liquid renormalization. The results for six different $Al/Al_2O_3/a$-Ga junctions were consistent and yielded a value for the Fermi-liquid parameter, G_0, of 0.81 ± 0.14. This corresponds to a decrease in the apparent Zeeman splitting near the phase boundary of 45% and graphically demonstrates the need to include Fermi-liquid effects in explaining the behavior of superconductors. We also found that the normal-state density of states in amorphous gallium was altered due to correlation effects. These effects were qualitatively those predicted by Altshuler and Aronov,[56] McMillan,[57] and

Altschuler, Aronov, and Lee.[58]

These results demonstrate the efficacy of determining the intrinsic Fermi-liquid parameters of a material from its superconducting properties. It was also found that the magnitude of the Fermi-liquid parameter G_0 could be accurately predicted from knowledge of its constituent interactions using the simple relation

$$1+G_0=(1+\lambda_{e\text{-ph}}+\lambda_s)(1-\bar{I}) .$$

Finally, these techniques were found to yield a value for the spin-orbit scattering parameter, $b_{\rm SO}^{a\text{-Ga}}=0.18\pm0.03$, which is fairly close to that predicted by a simple calculation.

ACKNOWLEDGMENTS

The authors wish to thank J. S. Moodera for many helpful discussions, J. E. Tkaczyk for the use of his computer program in digitizing their data, R. MacNabb for his help in the initial preparation of samples, and M. Blaho for his help in setting up test equipment. This work was supported by Air Force Office of Scientific Research (AFOSR) Contract No. F49620-85-C-0005.

*Present address: University of California–San Diego, Dept. of Physics, B-019, La Jolla, CA 92093.

[1]L. D. Landau, Zh. Eksp. Teor. Fiz. **30**, 1058 (1956) [Sov. Phys.—JETP **3**, 920 (1957)].

[2]L. D. Landau, Zh. Eksp. Teor. Fiz. **35**, 95 (1958) [Sov. Phys.—JETP **8**, 70 (1959)].

[3]B. R. Whiting, N. S. Vander Ven, and R. T. Schumacher, Phys. Rev. B **18**, 5413 (1978).

[4]G. L. Dunifer, D. Pinkel, and S. Schultz, Phys. Rev. B **10**, 3159 (1974).

[5]L. D. Flesner and S. Schultz, Phys. Rev. B **14**, 4759 (1976).

[6]D. Pinkel and S. Schultz, Phys. Rev. B **18**, 6639 (1978).

[7]C. E. Witt and N. S. Vander Ven, Phys. Rev. B **19**, 887 (1979).

[8]J. R. Sambles, D. A. H. Mace, and G. L. Dunifer, Pys. Rev. B **31**, 7408 (1985).

[9]D. L. Randles, Proc. R. Soc. London, Ser. A **331**, 85 (1972).

[10]B. Knecht, J. Low Temp. Phys. **21**, 619 (1975).

[11]J. M. Perz and D. Schoenberg, J. Low Temp. Phys. **25**, 275 (1976).

[12]W. M. Bibby and D. Shoenberg, J. Low Temp. Phys. **34**, 659 (1979).

[13]P. M. Platzman and P. A. Wolff, in *Waves and Interactions in Solid State Plasmas,* Suppl. 13 of *Solid State Physics: Advances in Research and Applications,* edited by F. Seitz and D. Turnbull (Academic, New York, 1973).

[14]D. C. Vier, D. W. Tolleth, and S. Schultz, Phys. Rev. B **29**, 88 (1984).

[15]A. M. Clogston, Phys. Rev. **125**, 439 (1962).

[16]T. P. Orlando, E. J. McNiff, Jr., S. Foner, and M. R. Beasley, Phys. Rev. B **19**, 4545 (1979).

[17]T. P. Orlando and M. R. Beasley, Phys. Rev. Lett. **46**, 1598 (1981).

[18]N. R. Werthamer, E. Helfand, and P. C. Hohenberg, Phys. Rev. **147**, 295 (1966).

[19]K. Maki, Phys. Rev. **148**, 362 (1966).

[20]P. Fulde, Adv. Phys. **22**, 667 (1973).

[21]R. C. Bruno and B. B. Schwartz, Phys. Rev. B **8**, 3161 (1973).

[22]P. M. Tedrow and R. Meservey, Phys. Rev. Lett. **43**, 384 (1979).

[23]P. M. Tedrow and R. Meservey, Phys. Rev. B **25**, 171 (1982).

[24]P. M. Tedrow, J. T. Kucera, D. Rainer, and T. P. Orlando, Phys. Rev. Lett. **52**, 1637 (1984).

[25]J. A. X. Alexander, T. P. Orlando, D. Rainer, and P. M. Tedrow, Phys. Rev. B **31**, 5811 (1985).

[26]One can think of these renormalized quasiparticles as Fermi-liquid excitations, or Fermi-liquid quasiparticles, made up from the traditional superconducting quasiparticles.

[27]T. T. Chen, J. T. Chen, J. D. Leslie, and H. J. T. Smith, Phys. Rev. Lett. **22**, 526 (1969).

[28]J. E. Jackson, C. V. Briscoe, and H. Wühl, Physica **55**, 447 (1971).

[29]G. Bergmann, Phys. Rev. B **7**, 4850 (1973).

[30]M. Dayan, J. Low Temp. Phys. **32**, 643 (1978).

[31]W. Bückel and R. Hilsch, Z. Phys. **138**, 109 (1954).

[32]R. W. Cohen, B. Abeles, and G. S. Weisbarth, Phys. Rev. Lett. **18**, 336 (1967).

[33]H. Wuhl, J. E. Jackson, and C. V. Briscoe, Phys. Rev. Lett. **20**, 1496 (1968).

[34]G. V. Minnigerode and J. Rothenberg, Z. Phys. **213**, 397 (1968).

[35]D. G. Naugle and R. E. Glover, Phys. Lett. **28A**, 611 (1969).

[36]J. D. Leslie, J. T. Chen, and T. T. Chen, Can. J. Phys. **48**, 2783 (1970).

[37]R. Meservey, P. M. Tedrow, and R. C. Bruno, Phys. Rev. B **11**, 4224 (1975).

[38]P. M. Tedrow and R. Meservey, Phys. Lett. **51A**, 57 (1975).

[39]J. Feder, S. R. Kiser, F. Rothwarf, J. P. Burger, and C. Valette, Solid State Commun. **4**, 611 (1966).

[40]H. Parr and J. Feder, Phys. Rev. B **7**, 166 (1973).

[41]A. J. Leggett, Phys. Rev. **140**, A1869 (1965).

[42]A. J. Leggett, Ann. Phys. (N.Y.) **46**, 76 (1968).

[43]A. J. Leggett, Rev. Mod. Phys. **47**, 331 (1975).

[44]G. Eilenberger, Z. Phys. **214**, 195 (1968).

[45]A. I. Larkin and Yu. N. Ovchinnikov, Zh. Eksp. Teor. Fiz. **55**, 2262 (1968) [Sov. Phys.—JETP **28**, 1200 (1969)].

[46]J. W. Serene and D. Rainer, Phys. Rep. **101**, 221 (1983).

[47]In general, away from the phase boundary, $H_{\rm int}=H_{\rm ext}[-G_0Y(t)/1+G_0Y(t)]$, where $Y(t)$ is the Yosida function (see Ref. 43). The Yosida function equals one for $t=T/T_c(H)\geq 1$ and decreases monotonically to zero as t drops to zero.

[48]J. A. X. Alexander, Ph.D. thesis, Massachusetts Institute of Technology, 1986 (unpublished).

[49]See, for example, E. L. Wolf, *Principles of Electron Tunneling Spectroscopy* (Oxford, New York, 1985).

[50]P. M. Tedrow, J. S. Moodera, and R. Meservey, Solid State Commun. **44**, 587 (1982).

[51]G. A. Gibson, and R. Meservey (unpublished).

[52]R. C. Dynes, V. Narayanamurti, and J. P. Garno, Phys. Rev. Lett. **41**, 1509 (1978).

[53]R. C. Dynes, J. P. Garno, G. B. Hertel, and T. P. Orlando, Phys. Rev. Lett. **53**, 2437 (1984).

[54]D. A. Browne, K. Levin, and K. A. Muttalib, Phys. Rev. Lett. **58**, 156 (1987).

[55]V. M. Kuz'menko, V. I. Mel'nikov, and V. A. Rakhubovskii, Zh. Eksp. Teor. Fiz. **86**, 1049 (1984) [Sov. Phys.—JETP **59**, 612 (1984)].

[56]B. L. Altschuler and A. G. Aronov, Zh. Eksp. Teor. Fiz. **77**,

2028 (1979) [Sov. Phys.—JETP **50**, 968 (1979)].

[57]W. L. McMillan, Phys. Rev. B **24**, 2739 (1981).

[58]B. L. Altschuler, A. G. Aronov, and P. A. Lee, Phys. Rev. Lett. **44**, 1288 (1980).

[59]D. Rainer, G. Bergmann, and U. Eckhardt, Phys. Rev. B **8**, 5354 (5354).

[60]The value 1.67 is coincidental; we are not observing surface sheath superconductivity. The parallel critical field has a square-root dependence on temperature near T_c.

[61]The Stoner factor gives the renormalization of the Pauli susceptibility due to electron-electron interactions: $\chi_P^* = \chi_P / (1-\bar{I})$.

[62]Using the theory of Berk and Schrieffer [Phys. Rev. Lett. **17**, 433 (1966)], Jensen and Andres [Phys. Rev. **165**, 545 (1968)] have shown that the renormalization of the effective mass of the quasiparticles due to the electron-phonon and paramagnon interactions is given by $m^*/m = 1+\lambda_{e\text{-ph}}+\lambda_s$. Berk and Schrieffer's theory can also be used to show that in the static, long-wavelength limit the spin susceptibility is given by $\chi(0,0) = 2\mu_B^2 N_0/[1-\bar{I}]$. In terms of the Fermi-liquid theory the spin susceptibility is given by

$$\chi = 2\mu_B^2 (m^*/m) N_0/(1+G_0)$$

[see, for example, J. W. Wilkins, in *Electrons at the Fermi Surface,* edited by M. Springford (Cambridge University Press, London, 1980)] Combining these results yields Eq. (4). Equation (4) has also been suggested by Orlando and Beasley [Phys. Rev. Lett. **46**, 1598 (1981)].

[63]P. B. Allen and R. C. Dynes, Phys. Rev. B **12**, 905 (1975).

[64]J. M. Daams, B. Mitrović, and J. P. Carbotte, Phys. Rev. Lett. **46**, 65 (1981).

[65]M. A. Jensen and K. Andres, Phys. Rev. **165**, 545 (1968).

[66]C. R. Leavens and A. H. MacDonald, Phys. Rev. B **27**, 2812 (1983).

[67]D. Rainer (private communication).

[68]W. Gallagher, Ph.D. thesis, Massachusetts Institute of Technology, 1978 (unpublished). The spin-orbit scattering rate may itself be renormalized by Fermi-liquid interactions. We use Eq. (6) only as a rough estimate for b_{SO}.

[69]L. D. Landau and E. M. Lifshitz, *Quantum Mechanics* (Pergamon, New York, 1977), Sec. 72.

[70]H. J. Zeiger and G. W. Pratt, *Magnetic Interactions in Solids* (Clarendon, Oxford, 1973), p. 36.

[71]A. A. Abrikosov and L. P. Gorkov, Zh. Eksp. Teor. Fiz. **42**, 1088 (1962) [Sov. Phys.—JETP **15**, 752 (1962)].

[72]Y. Yafet, Solid State Phys. **14**, 1 (1963).

[73]R. Meservey and P. M. Tedrow, Phys. Rev. Lett. **41**, 805 (1978). The authors have shown empirically that spin-orbit scattering occurs predominately at surfaces in thin films, and that for a large number of elements $b_{SO} \sim Z^4$.

[74]The use of the free-electron model is justified by the fact that the structure of *a*-Ga is like that of liquid metals, as shown by x-ray diffraction [W. Bückel, Z. Phys. **138**, 136 (1954)]. Furthermore, Bergmann [Z. Phys. **255**, 76 (1972)] has measured the Hall effect constant for *a*-Ga and found good agreement with the free-electron model.

[75]J. E. Tkaczyk, Ph.D. thesis, Massachusetts Institute of Technology, 1988 (unpublished).